HIGH RESOLUTION SPECTROSCOPY OF RED GIANT BRANCH STARS AND THE CHEMICAL EVOLUTION OF THE FORNAX DWARF SPHEROIDAL GALAXY

B. Lemasle[1], T.J.L. de Boer[2], V. Hill[3], E. Tolstoy[4], M. J. Irwin[2], P. Jablonka[5,6], K. Venn[7], G. Battaglia[8,9], E. Starkenburg[7,10], M. Shetrone[11], B. Letarte[12], P. Francois[6,13], A. Helmi[4], F. Primas[14], A. Kaufer[15] and T. Szeifert[15]

Abstract. From VLT-FLAMES high-resolution spectra, we determine the abundances of several α, iron-peak and neutron-capture elements in 47 Red Giant Branch stars in the Fornax dwarf spheroidal galaxy. We confirm that SNe Ia started to contribute to the chemical enrichment of Fornax at [Fe/H] between –2.0 and –1.8 dex. Combining these abundances with accurate age estimates, we date the onset of SNe Ia to $\approx$ 12–10 Gyrs ago. Our results are compatible with an initial mass function that lacks the most massive stars and with a star formation going on throughout the whole history of Fornax.

Keywords: stars: abundances, galaxies: individual: Fornax dwarf spheroidal, galaxies: evolution

1 Introduction

The wide variety of Star Formation Histories (SFH) observed in Local Group dwarf spheroidal galaxies (dSphs) makes them an ideal laboratory for studying the physical processes driving the evolution of galaxies. In addition, they provide valuable clues on the formation and evolution of our own Milky Way. Fornax is one of the most luminous and most massive dSphs (Mateo 1998). If star formation was going on over almost its entire history (e.g., de Boer et al. 2012b), Fornax is nevertheless dominated by its intermediated age population, in particular a 4 Gyr old population at [Fe/H] $\approx$ –1.0 dex. We have studied the chemical evolution of Fornax by determining the abundances of several α, iron peak and n-capture elements in 47 Red Giant Branch (RGB) stars $\approx$0.4 degrees offset from the centre of the galaxy and covering the whole metallicity range. We also derived accurate ages from the age probability distribution from the colour-magnitude diagram of Fornax.

---

[1] Anton Pannekoek Institute, University of Amsterdam, Science Park 904, PO Box 94249, 1090 GE, Amsterdam, The Netherlands

[2] Institute of Astronomy, University of Cambridge, Madingley Road, Cambridge, CB3 0HA, UK

[3] Observatoire de la Côte d'Azur, CNRS UMR 7293, BP4229, 06304, Nice Cedex 4, France

[4] Kapteyn Astronomical Institute, University of Groningen, Postbus 800, 9700 AV, Groningen, The Netherlands

[5] Laboratoire d'astrophysique, École Polytechnique Fédérale de Lausanne (EPFL), Observatoire de Sauverny, 1290 Versoix, Switzerland

[6] GEPI, Observatoire de Paris, CNRS, Université Paris Diderot, Place Jules Janssen, 92190 Meudon, France

[7] Department of Physics and Astronomy, University of Victoria, 3800 Finnerty Road, Victoria, BC, V8P 1A1, Canada

[8] Istituto de Astrofisica de Canarias, calle via Lactea s/n, 38205 San Cristobal de La Laguna (Tenerife), Spain

[9] Universidad de La Laguna, Dpto. Astrofsica, E-38206 La Laguna, Tenerife, Spain

[10] CIFAR Global Scholar

[11] McDonald Observatory, The University of Texas at Austin, 1 University Station, C1400, Austin, TX 78712-0259, USA

[12] Dept of Physics, North-West University, Mafikeng Campus, Private Bag X2046, Mmabatho 2745, South Africa

[13] UPJV, Université de Picardie Jules Verne, 33 rue St. Leu, 80080 Amiens, France

[14] European Southern Observatory, Karl Schwarzschild Str. 2, 85748, Garching b. München, Germany

[15] European Southern Observatory, Alonso de Cordova 3107, Santiago, Chile

2   Data and analysis

We obtained FLAMES/GIRAFFE high resolution (HR) spectra using the HR10, HR13 and HR14 gratings for 47 RGB stars. Most of them were selected for membership from low resolution spectra in the calcium triplet (CaT) region (Battaglia et al. 2006) while the remaining stars were selected from their position on the (I, V-I) CMD (Battaglia et al. 2006, ESO/WFI).

We determined both the radial velocities (V_r) and the equivalent widths of the absorption lines with the DAOSPEC software (Stetson & Pancino 2008). From a Gaussian fit to the data, we derived a systematic radial velocity peak of 49.65±1.46 km s^{-1}, σ=14.6±1.51 km s^{-1}. This value falls below previous determinations over the whole galaxy from CaT (Battaglia et al. 2006, V_r=54.1±0.5 km s^{-1}, σ=11.4±0.4 km s^{-1}) or magnesium triplet (Walker et al. 2009, V_r=55.2±0.1 km s^{-1}, σ=11.7±0.9 km s^{-1}); or in the centre of Fornax from high resolution spectra (Letarte et al. 2010, V_r=55.9 km s^{-1}, σ=14.2 km s^{-1}) If we select the Fornax members that overlap our HR sample in the CaT data of Battaglia et al. (2006), we find a similar mean radial velocity (50.99±0.94 km s^{-1}, σ=12.70±0.96 km s^{-1}). This indicates that slightly lower V_r are typical from this region of Fornax and suggests that the kinematics of Fornax depends on position.

We used a grid of OSMARCS atmosphere models in spherical symmetry (Gustafsson et al. 2008) with [α/Fe] increasing when [Fe/H] decreases and computed abundances with *calrai*, a LTE spectrum synthesis code originally developed by Spite (1967) and regularly updated since then. Both temperature and surface gravities are computed from photometric data. T_{eff} is the average of the temperatures derived from the five different colours (B-V), (V-I), (V-J), (V-H) and (V-K), and the calibration for giants from Ramìrez & Meléndez (2005). Surface gravities *log g* are derived using our temperature estimates, a distance modulus of μ_v=20.84±0.04 mag (Pietrzyński et al. 2009) and the bolometric correction from Alonso et al. (1999), Different stellar masses ranging from 0.9 to 1.3 $M_\odot$ are assigned to the stars depending on their metallicity. We checked the photometric T_{eff} by ensuring that [FeI/H] does not depend on the excitation potential χ_{ex} and obtained the value of the microturbulent velocity v_t by requiring that [FeI/H] does not depend on EW.

To determine the ages of an individual RGB star, a global synthetic CMD of Fornax is first built from the SFH (de Boer et al. 2012a). All the stars with the same magnitude and the same metallicity (within the observational uncertainties) are then extracted from the synthetic CMD and the mean age and the standard deviation of this subsample are adopted respectively as the age of the individual RGB star and its associated uncertainty. To take into account population gradients within Fornax, the SFH is computed in 5 different annuli at different distances from the centre of Fornax.

3   Results and discussion

3.1   The classical time-delay scenario

The left panel of Fig. 1 shows that the old, metal-poor stars of Fornax are typically Mg-rich while the young metal-rich stars are Mg-poor. The same outcome applies to the other α-elements, in particular Si and Ca (not shown here). Such a feature is also observed in other dSphs. In a now traditional interpretation (e.g. Tinsley 1979; Matteucci 2003), the low [α/Fe] in the dSphs are believed to originate in the time delay between type II and type Ia Supernovae (respectively SNe II and SNe Ia): SNe II are the main contributor to the enrichment of the interstellar medium (ISM) in α-elements and because of their short timescale, the ISM is enriched by the massive stars very rapidly after the beginning of star formation. In contrast, SNe Ia contribute only later to the chemical enrichment and their onset leads to low [α/Fe] values.

In this scenario, the evolution of [Mg/Fe] with [Fe/H] (Fig. 1, left panel) indicates that the Mg "knee" where [Mg/Fe] turns down after the onset of SNe Ia took place at [Fe/H] between –2.0 and –1.8 dex. This result perfectly matches the value of –1.9 dex recently found by Hendricks et al. (2014). From the evolution of [Mg/Fe] with age (Fig. 1, right panel) we find that the [Mg/Fe] knee occurred approximately between 12–10 Gyrs ago.

These values are similar to those recently found for the Sculptor dSph where the Mg knee takes place at 10.9±1.0 Gyr and at a metallicity of ≈–1.8 dex (Tolstoy et al. 2009; de Boer et al. 2012a). Because SF efficiency scales with galaxy mass, it was expected that Fornax (~10 times more massive than Sculptor) produces more metals and keeps a larger fraction of them. Indeed several observational evidences argue against strong galactic winds, for instance the continuous SFH, the steady decline in [Mg/Fe] or the high values of the [Ba/Fe] and [La/Fe], the latter two indicating that the Asymptotic Giant Branch (AGB) yields have not been lost.
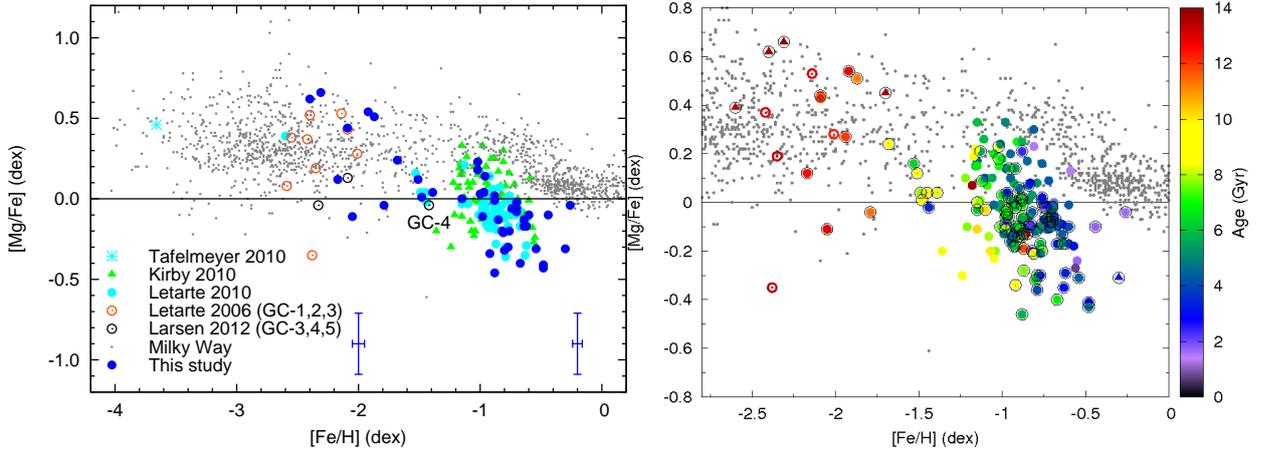
Fig. 1. Left: The distribution of [Mg/Fe] for our sample of RGB stars in the Fornax dSph as blue filled circles. The cyan filled circles are the data of Letarte et al. (2010) and the cyan triangle the metal-poor star of Tafelmeyer et al. (2010). The orange open circles are the stars in Fornax globular clusters from Letarte et al. (2006). We also show the stars from the medium resolution sample of Kirby et al. (2010) that have uncertainties in [Fe/H] and [Mg/H] lower than 0.2 dex and that are not included in the HR samples. Milky Way halo stars from Venn et al. (2004) and Frebel (2010) and references therein are in small grey dots. Representative error bars are given for the metal-poor ([Fe/H]<−1.4 dex) and metal-rich ([Fe/H]>−1.4 dex) regimes. **Right:** [Mg/Fe] vs [Fe/H] from MR/HR spectroscopic measurements of Fornax RGB stars (coloured filled circles/triangles). The colours represent the age in Gyr, derived from the SFH. Stars in the Milky Way are shown for comparison (small grey points). Field stars for which the probability distribution for age could be determined are shown as filled circles, while filled triangles show stars for which no statistical age estimate could be derived. For those stars, only an age estimate is given, based on the closest distance from synthetic CMD satisfying the magnitude and metallicity constraints. Globular cluster stars are shown as open circles. Stars belonging to the high resolution samples (this study, Letarte et al. 2010) are surrounded by black open circles.

A merger scenario is then very attractive: with a low original mass, Fornax could experience an early enrichment similar to Sculptor and reach its current higher mass via a merger event. Such a scenario has already been proposed by several authors: based on kinematics, Amorisco & Evans (2012c) suggested that Fornax is the outcome of the late merger of a bound pair. In a successfull attempt to recover the shell-like substructures that can be found in Fornax (e.g., de Boer et al. 2013, and references therein), Yozin & Bekki (2012) proposed a merger event with a low-mass companion (5% of the Fornax mass) that occured between 3.5 and 2.1 Gyr ago. On the other hand, recent collision between Milky Way satellites are much less probable than it was at the early times of the Local Group (e.g., De Rijcke et al. 2004)

3.2 A top-light IMF ?

A steep (or "top-light") initial mass function has often been proposed for dwarf galaxies (e.g., Tolstoy et al. 2003; Kroupa et al. 2013). As far as Fornax is concerned, the case was advocated by Tsujimoto (2011) with a detailed model of the galaxy and by Li et al. (2013a) when comparing the nucleosynthesis in the Milky Way and in Fornax. Analysing RGB stars in Sagittarius (a dSph with a mass similar to Fornax), McWilliam et al. (2013) conclude that the low [α/Fe] observed are not the result of the time-delay scenario but rather the outcome of a top-light IMF where the most massive stars (>30 M⊙) are missing. Indeed, the production of O and Mg is dominated by the most massive SNe II (Woosley & Weaver 1995). McWilliam et al. (2013) also proposed that the r-process elements are mostly originating from low mass SNe II, providing a very straightforward explanation for the supersolar [Eu/Mg] we find in Fornax in the case of a top-light IMF. Other results like low values of [Ni/Fe], high values of [Ba/Fe] underline the strong influence of SNe Ia and AGB stars in driving the abundance pattern of Fornax and are therefore compatible with a steep IMF.

However it is important to note that most of these studies considered only the metal-rich regime of Fornax or Sagittarius. Moreover, the presence of globular clusters in both these galaxies indicates that in the early times, gas was present in large enough quantities to form the largest molecular clouds and in turn the most

massive stars (Oey 2011). This seems to contradict the steep IMF hypothesis, which is the natural outcome of systems where gas is not present in sufficient quantities.

4   Conclusions

We confirm that in Fornax, SNe Ia started to contribute to the chemical enrichment of the ISM at [Fe/H] between –2.0 and –1.8 dex. We find that the onset of SNe Ia took place ≈12–10 Gyrs ago. These value are similar to those reported for the Sculptor dSph despite the fact that Fornax is much more massive than Sculptor. Low [Mg/Fe], supersolar [Eu/Mg] suggest a top-light IMF in Fornax. Low [Ni/Fe], high [Ba/Fe] in the metal-rich regime reflect the strong influence of SNe Ia and AGB stars in the abundance pattern of Fornax. The time-delay and the top-light IMF scenarios are not mutually exclusive and are probably going on simultaneously in Fornax.

References

Alonso, A., Arribas, S., Martínez-Roger, C. 1999, A&AS 140, 261

Amorisco, N. C., Evans, N. W., 2012, ApJ 756, 2

Battaglia, G., Tolstoy, E., Helmi, A., Irwin, M. J., Letarte, B., Jablonka, P., Hill, V., Venn, K. A., Shetrone, M. D., Arimoto, N., Primas, F., Kaufer, A., François, P., Szeifert, T., Abel, T., Sadakane, K., 2006, A&A 459, 423

de Boer, T. J. L., Tolstoy, E., Hill, V., Saha, A., Olsen, K., Starkenburg, E., Lemasle, B., Irwin, M. J., Battaglia, G., 2012, A&A 539, A103

de Boer, T. J. L., Tolstoy, E., Hill, V., Saha, A., Olszewski, E. W., Mateo, M., Starkenburg, E., Battaglia, G., Walker, M. G., 2012, A&A 544, A73

de Boer, T. J. L., Tolstoy, E., Saha, A., Olszewski, E. W., 2013, A&A 551, A103

De Rijcke, S., Dejonghe, H., Zeilinger, W. W., Hau, G. K. T., 2004, A&A, 426, 53

Frebel, A., 2010, AN 331, 474

Gustafsson, B., Edvardsson, B., Eriksson, K., Jørgensen, U. G., Nordlund, Å., Plez, B., 2008, A&A 486, 951

Hendricks, B., Koch, A., Lanfranchi, G. A., Boeche, C.,Walker, M., Johnson, C. I., Penarrubia, J., Gilmore, G., 2014, ApJ 785, 102

Kirby, E. N., Guhathakurta, P., Simon, J. D., Geha, M. C., Rockosi, C. M., Sneden, C., Cohen, J. G., Sohn, S. T., Majewski, S. R., Siegel, M., 2010, ApJ SS 191, 352

Kroupa, P., Weidner, C., Pflamm-Altenburg, J., Thies, I., Dabringhausen, J., Marks, M., Maschberger, T., 2013

Letarte, B., Hill, V., Jablonka, P., Tolstoy, E., François, P., Meylan, G., 2006, A&A 453, 547

Letarte, B., Hill, V., Tolstoy, E., Jablonka, P., Shetrone, M., Venn, K. A., Spite, M., Irwin, M. J., Battaglia, G., Helmi, A., Primas, F., François, P., Kaufer, A., Szeifert, T., Arimoto, N., Sadakane, K., 2010, A&A 523, A17

Li, H., Cui, W., Zhang, B., 2013a, ApJ 775, 12

Mateo, M., 1998, ARA&A 36, 435

Matteucci, F., 2003, Ap&SS 284, 539

McWilliam, A., Wallerstein, G., Mottini, M., 2013, ApJ 778, 149

Oey, M. S., 2011, ApJL 739, 46

Pietrzyński, G., Górski, M., Gieren, W., Ivanov, V. D., Bresolin, F., Kudritzki, R-P., 2009, AJ 138, 459

Ramìrez, I., Meléndez, J., 2005, ApJ 626, 465

Spite, M., 1967, AnAp 30, 211

Stetson, P. B., Pancino, E., 2008, PASP 120, 1332

Tafelmeyer, M., Jablonka, P., Hill, V., Shetrone, M., Tolstoy, E., Irwin, M. J., Battaglia, G., Helmi, A., Starkenburg, E., Venn, K. A., Abel, T., François, P., Kaufer, A., North, P., Primas, F., Szeifert, T., 2010, A&A 524, A58

Tinsley, B. M., 1979, ApJ 229,1046

Tolstoy, E., Venn, K. A., Shetrone, M., Primas, F., Hill, V., Kaufer, A., Szeifert, T., 2003, AJ 125, 707

Tolstoy, E., Hill, V., Tosi, M., 2009, ARA&A 47, 371

Tsujimoto, T., 2011, ApJ 778, 149

Venn, K. A., Irwin, M., Shetrone, M. D., Tout, C. A., Hill, V., Tolstoy, E., 2004, AJ 128, 1177

Walker, M. G., Mateo, M., Olszewski, E. W., Sen, B., Woodroofe, M., 2009, AJ 137, 3109

Woosley, S. E., Weaver, T. A., 1995, ApJS 101, 181

Yozin, C., Bekki, K., 2012, ApJ 756, 18